

# Local Magnetic Fields in the Pinned Vortex State: Effect on the $\mu^+$ -Spin-Rotation Line Shape

D. R. Harshman, A. T. Fiory, and R. J. Cava

AT&T Bell Laboratories, Murray Hill, New Jersey 07974

(Received 2 October 1990)

Local-magnetic-field distributions in the superconducting mixed state of high- $T_c$  cuprates were measured by muon-spin rotation ( $\mu$ SR) in the absence of applied driving forces. In this first analytical treatment, a critical-state model, incorporating an anisotropic penetration depth  $[\lambda_{ab}(0) = 1300 \pm 100 \text{ \AA}]$  in the basal plane], reveals the strong influence of local pinning on the characteristic shape of low-temperature  $\mu$ SR Fourier spectra for  $\text{YBa}_2\text{Cu}_3\text{O}_7$ . The linewidths are found to be nearly independent of flux density, indicative of noncollective or local pinning.

PACS numbers: 74.70.Vy, 74.60.Ge, 76.75.+i

Interest in vortex states of high- $T_c$  superconductors has been heightened by various predictions of fluid, polymeric, glassy, or lattice topologies, based largely on the premise of weak or dilute elementary pinning forces and justified by observations of vanishing critical current at high temperatures.<sup>1-4</sup> However, many experiments are also consistent with conventional pictures of flux pinning and thermal activation,<sup>5</sup> examples of which are observed in the quasistatic magnetization of  $\text{YBa}_2\text{Cu}_3\text{O}_7$ .<sup>6,7</sup> Since the distinction lies in the detailed collective behavior, it is evident that direct and microscopic observations of vortex distributions are important. To this end, we have applied the muon-spin-rotation ( $\mu$ SR) technique<sup>8</sup> and focus attention on the vortex configuration produced at low temperature by cooling in a constant external field  $\mathbf{H}_{\text{ext}}$ . Ideally, field cooling is the least perturbative procedure for nucleating vortices, initially in fluidlike configurations, and approaching equilibrium in a frozen glassy or lattice state. Since our objective is to ascertain the importance of vortex pinning in this scenario, we have studied a sintered ceramic sample of  $\text{YBa}_2\text{Cu}_3\text{O}_7$ , chosen for its low microscopic disorder and weak flux pinning. Comparison of the Bean critical-state model<sup>9</sup> to the non-Gaussian, asymmetric peaks in the  $\mu^+$ SR Fourier spectra shows good agreement, indicating that the vortex distribution produced by field cooling is dominated by pinning. Since the linewidths are weakly dependent on  $H_{\text{ext}}$ , it appears that collective vortex interactions do not play a significant role in the pinning mechanism.

Implicit in the interpretation of time-differential  $\mu$ SR spectra is the assumption that the  $\mu^+$  sample random sites, yielding a spin-relaxation function of time,  $G(t)$ , whose Fourier transform gives the probability distribution of local magnetic fields,  $P(B)$ .<sup>8</sup> An earlier demonstration of the method, applied to single crystals of Nb, showed that  $P(B)$  is close to the theoretical local-magnetic-field distribution in the vortex lattice,  $P_c(B)$ .<sup>10</sup> While  $\mu$ SR in high- $T_c$  superconductors has been successful in determining the pairing state and penetration depth,<sup>11</sup> confirming theory for  $P_c$  for an anisotropic penetration depth has thus far proved to be elusive.

Surface-decoration experiments, limited to weak magnetic fields, were the first to confirm triangular short-range ordering, to determine the penetration-depth anisotropy, and to indicate a high density of pinning sites.<sup>12</sup> The majority of experiments have employed polycrystalline materials prepared by a ceramic process, which permits good control over composition and structure, and have fitted  $G(t)$  with a simple form such as a Gaussian. Inspection of the corresponding Fourier transforms, however, indicates asymmetric peaks in  $P(B)$  rather than a symmetric Gaussian.<sup>13,14</sup> A direct approach for extracting the basal-plane components of the London penetration depth,  $\lambda_{ab} \equiv (\lambda_a \lambda_b)^{1/2}$ , based on fitting  $G(t)$ , with model functions approximating the theoretical depolarization,<sup>15</sup> was applied to single crystals of the  $T_c = 90$  and 60 K phases of  $\text{YBa}_2\text{Cu}_3\text{O}_7$ , yielding  $\lambda_{ab} = 1415$  and 2250  $\text{\AA}$ , respectively.<sup>11</sup>

Numerical evaluation of  $P_c(B)$  for uniform vortex lattices in a uniaxial superconductor is shown in Fig. 1,

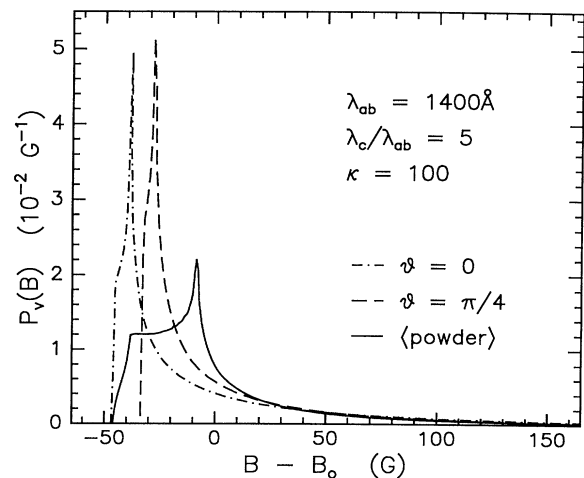


FIG. 1. Theoretical muon local-magnetic-field distributions  $P_c(B)$  for a uniaxial superconductor in the mixed state for  $c$  axis at angles 0,  $\pi/4$ , or randomly averaged orientation with respect to external field.

with curves computed for angles  $\theta$  between the  $c$  axis and  $\mathbf{H}_{\text{ext}}$  taken as 0,  $\pi/4$ , or randomly averaged (powder).<sup>16</sup> These represent ideal models for  $\text{YBa}_2\text{Cu}_3\text{O}_7$  at low temperature, in terms of  $\lambda_{ab}=1400$  Å, anisotropy ratio  $\lambda_c/\lambda_{ab}=5$ , Ginzburg-Landau parameter  $\kappa=100$ , and  $H_{c1}\ll H_{\text{ext}}\ll H_{c2}$ . For a given anisotropy ratio, the width of  $P_c(B)$  scales as  $\lambda_{ab}^{-2}$ . The average magnetic induction,  $B_0=N\phi_0$ , is determined by the vortex-lattice areal density  $N$  and  $\phi_0=hc/2e$ . At  $0<\theta<\pi/2$ ,  $\mathbf{B}$  is not parallel to  $\mathbf{H}_{\text{ext}}$ ,<sup>17</sup> but the misalignment is imperceptible for typical  $B_0$  large compared to the width of  $P_c(B)$ . Tilting the  $c$  axis away from the applied field distorts the triangular cell of the vortex lattice from equilateral to isosceles and reduces the local-field variation.<sup>17</sup> For increasing  $\theta$ , the Van Hove cusp shifts towards the peak in the powder curve. A larger anisotropy ratio shifts the peak in the powder curve towards  $B_0$ , leaving unchanged the edge coincident with the cusp at  $\theta=0$ . The salient features of the powder curve, referred to in the following discussion of the data, are the steep cutoff at low field and the broad tail extending to the maximum field in the vortex cores.

The effect of lattice disorder can be obtained through a convolution of the ideal  $P_c(B)$  with a suitable broadening function  $F(B)$ . Disordering of vortex lattices by random pinning forces and by thermal vibration have been treated theoretically,<sup>10</sup> where it was found that the smearing of  $P_c(B)$  is most pronounced in the high-field tail, owing to disordering of the core positions. Since the tail contributes little weight,  $F(B)$  for a vortex glass or amorphous state could be approximated by a Gaussian function.

Given the distribution of sizes, shapes, orientations, and connectedness among grains in ceramic specimens, a distribution in local demagnetizing fields is also to be expected.<sup>18</sup> In the field-cooling method, vortices nucleate from a polarization of the fluctuation regime near the  $H_{c2}(T)=H_{\text{ext}}$  phase boundary. If the vortices were to form a fluid, then it would freely expand on cooling, as flux is driven outward by diamagnetic screening currents, until the irreversibility temperature is reached. The equilibrium magnetic induction within the grains at low temperature would be on the order of  $10^2$  G lower than the external field, in the absence of pinning, and vary with grain orientation and shape.<sup>17</sup> Critical-state studies show that the grains decouple in strong magnetic fields, and that the irreversibility is dominated by pinning within the grains.<sup>19</sup> In  $\text{YBa}_2\text{Cu}_3\text{O}_7$  ceramics the irreversibility is already about 10% of the reversible magnetization at  $T=77$  K.

In the Bean-model description of the critical state, based on a field-independent pinning force,  $B$  decreases linearly with distance from the center to the edge of the grains.<sup>9</sup> The macroscopic distribution in local induction within a single grain (assuming a cylindrical model) is given by  $f_g=2(B_0-B)(B^*)^{-2}$ , for  $B_0-B^*\leq B\leq B_0$ ,

where  $B^*=4\pi c^{-1}RJ_c$ ,  $R$  the grain radius,  $J_c$  the critical current density, and  $B_0$  the flux density trapped at the center of the grain. The magnitude of this effect can be estimated from magnetization experiments on single crystals, which show an approximate scaling of irreversible magnetic moment with crystal size.<sup>7</sup> For  $R=10$   $\mu\text{m}$  and  $J_c\sim 10^5$  Acm<sup>-2</sup>, one could expect  $B^*\approx 124$  G. Variations among grains in a ceramic specimen is incorporated in a simple manner by averaging  $f_g$  over a Gaussian distribution in  $B^*$ . The result is a flux-gradient distribution, expressed as

$$F_p=2^{3/2}\delta^{-1}[\pi^{-1/2}\exp(-b^2)-b\text{erfc}(b)],$$

for  $b\geq 0$ , where  $b=(B_0-B)/\delta$  and  $\delta$  is the width of the distribution in  $B^*$ . The final result, for the local-field distribution  $P(B)$ , is a convolution of  $F_p$  with the vortex local-field distribution which, in this ideal treatment, would be  $P_c$  of Fig. 1. This simplified flux-trapping model introduces a single parameter  $\delta$ , related to grain size and critical current density. Since pinning destroys lattice order, there is some additional random broadening of  $P_c$  as well.

To test the theoretical predictions of the flux-trapping model,  $\mu^+$ SR data were taken on a phase-pure ceramic powder specimen of  $\text{YBa}_2\text{Cu}_3\text{O}_7$  (32-mm-diam  $\times$  3-mm-thick cylinder; grain-size distribution,  $35\pm 15$   $\mu\text{m}$ ) as ascertained by x-ray, resistivity, dc magnetization, and  $\mu$ SR analysis. Energetic (4.2 MeV) positive muons were implanted with spins polarized transverse to  $\mathbf{H}_{\text{ext}}$  (applied along the thin-sample dimension), and the oscillatory  $G(t)$  was determined from the spectrum of decay positrons ( $\mu^+\rightarrow e^++\bar{\nu}_\mu+\nu_e$ ). To smoothly truncate the finite time window of the experiment,  $G(t)$  was multiplied by a Gaussian envelope adding an effective 3.6 G to the linewidth resolution, prior to taking the Fourier transform. The experimental dead-time interval ( $0\leq t\lesssim 20$  ns) was filled by extrapolation and the phase angle was checked against measurements in the normal state.

Figure 2 shows the Fourier-transform spectrum (points),  $P(B)$ , obtained by field cooling to  $T=5$  K in  $H_{\text{ext}}=18$  kOe. Each panel presents a curve for a possible model of the broadening function  $F(B)$ , fitted to the data in convolution with the ideal theoretical  $P_c$  in a powder and for  $B_0$  as an adjustable parameter. In Fig. 2(a),  $P_c$  was broadened by a Gaussian of width  $\Delta B=4$  G, to take into account the smoothing of the experimental data, and was fitted with  $\lambda_{ab}=910$  Å. Although the width apparent to the eye for this model curve matches the experimental width (half width at half maximum is 43 G), it is obvious that the experimental peak is substantially broadened and distorted compared to the ideal  $P_c$ . In Fig. 2(b),  $P_c$  was broadened by convolution with a Gaussian distribution in penetration depths; the fitting parameters obtained are  $\lambda_{ab}=910$  Å and width  $\Delta\lambda_{ab}=230$  Å. The motivation here was to place an upper limit on superconducting inhomogeneity, in view of the

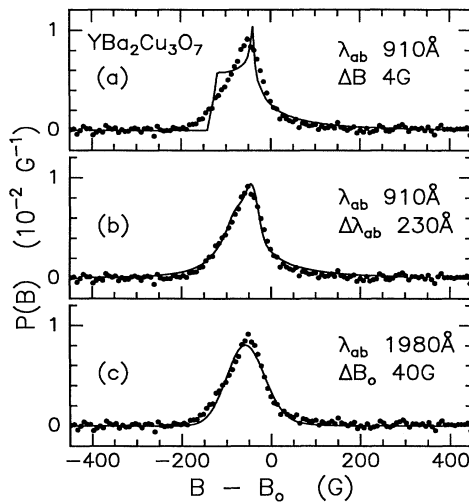


FIG. 2.  $\mu$ SR Fourier transform for  $\text{YBa}_2\text{Cu}_3\text{O}_7$  powder, obtained by cooling to  $T=5$  K in constant  $H_{\text{ext}}=18$  kOe, shown as points. Curves show powder theoretical  $P_c$ , for  $\lambda_c/\lambda_{ab}=5$ , convolved with Gaussian broadening: (a) instrumental broadening in  $B$ , (b) variation in  $\lambda_{ab}$ , and (c) variation in average induction  $B_0$ .

intrinsic nonsuperconducting inclusions predicted predicted for the cuprates.<sup>20</sup> In Fig. 2(c),  $P_c$  was broadened by convolution with a Gaussian distribution in  $B_0$ ; the fitting parameters are  $\lambda_{ab}=1980$  Å and width  $\Delta B_0=40$  G. Random variations in  $B_0$  are a model for the granular texture of the sample as well as random lattice disorder.

None of the broadening models presented in Fig. 2 accurately fits the data. Comparison of the fits in the  $B \gtrsim B_0$  region, which is sensitive to the value of  $\lambda_{ab}$ , shows that the proper value for  $\lambda_{ab}$  fall between the parameters from fits (b) and (c). Fitting the data with a simple Gaussian (not shown) gives a peak somewhat like that in Fig. 2(c). Important features of the experimental line shape yet to be explained are the cusp, which is sharper than a Gaussian peak, and its asymmetry, being notably shallower on the low-field side and steeper on the high-field side, as compared to Gaussian broadening. This asymmetry, actually opposite to that of the ideal  $P_c(B)$  distribution, points to the asymmetric magnetization inhomogeneity of the flux-trapping model, considered next. On cooling from above  $T_c$  to 5 K, the average muon precession frequency was found to exhibit a weak ( $-0.1$  MHz or  $-7$  G) shift, consistent with flux trapping.

Figure 3 shows field-cooling  $P(B)$  data taken at five values of  $H_{\text{ext}}$ . The data were shifted by an amount equal to the fitted parameter  $B_0$  to make evident the nearly invariant shape of the Fourier transforms. The widths fall in a  $\pm 7\%$  range. Since the theoretical distributions  $P_c$  are also nearly the same in this range of  $H_{\text{ext}}$

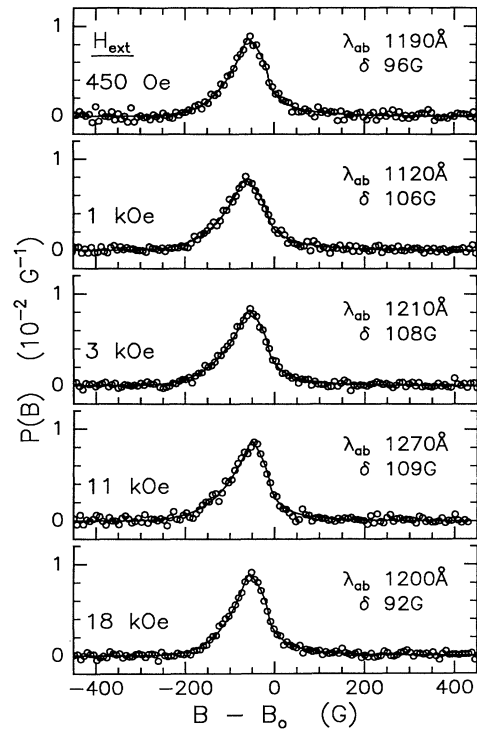


FIG. 3. Fourier-transform  $\mu$ SR local-field distributions at five values of  $H_{\text{ext}}$  indicated, offset by  $B_0 \approx H_{\text{ext}}$ . Solid curves are fits with the flux-trapping model discussed in the text. The penetration depths  $\lambda_{ab}$  and flux-pinning parameter  $\delta$  are given for each fitted curve.

(apart from the offset  $B_0$ ), the broadening mechanism must be field independent. The curves in Fig. 3 are fits with the flux-trapping model, derived above, where the powder  $P_c$  is convolved with the flux-gradient distribution function  $F_p$ . For each curve  $\delta$ ,  $\lambda_{ab}$ , and  $B_0$  were taken as adjustable parameters and the anisotropy ratio was fixed at 5 (larger anisotropy increases the result for  $\lambda_{ab}$  up to 2%). Clearly, the data are best described by the flux-trapping model, which accurately accounts for the cusplike peaks and reversed sense of the asymmetry, as compared to the models represented in Fig. 2.

The small variation in the  $\delta$  parameters indicates that the  $B^*$ , pertaining to pinning forces near equilibrium conditions, is not strongly field dependent. Collective pinning is expected to cause critical currents, hence  $B^*$  to decrease with flux density.<sup>21</sup> Since little field dependence is evident, we conclude that the vortices are trapped by elementary pinning forces, in which the density of pinning sites is high enough to mask any dependence on vortex density. A similar conclusion was drawn from decoration measurements in very weak magnetic fields.<sup>12</sup>

Contributions to line broadening from distortion of the vortex lattice and inhomogeneous magnetization have

not been included in the trapping model, because adding a random-width parameter is a minor improvement to the already very good fits in Fig. 3. The additional random width is about 20 G, which increases by  $\sim 10\%$  the value and systematic uncertainty in the penetration depth. The best estimates thus obtained are  $\lambda_{ab} = 1300 \pm 100$  Å and  $\delta \approx 95$  G. Although the model might be further refined by introducing the effects of anisotropic pinning,<sup>22</sup> vortex-lattice disorder, and grain distribution,<sup>18</sup> the essential conclusion, that of an asymmetric magnetic-field distribution caused by field gradients stabilized by local pinning, remains unaltered. A parallel  $\mu$ SR study of the  $T_c = 58$  K superconductor  $\text{YBa}_2\text{Cu}_3\text{O}_{6.65}$  was also performed, yielding qualitatively similar line shapes fitted with  $\lambda_{ab} \approx 2300$  Å and  $\delta \approx 35$  G.

In summary, we have demonstrated, by  $\mu$ SR analysis, the sensitivity of the vortex state in high- $T_c$  superconductors to disorder caused by local flux pinning. This is revealed as field-independent broadening near equilibrium, which is to be contrasted to field-dependent collective pinning observed in conventional forced-response studies.<sup>21</sup> A critical-state model for flux trapping and penetration-depth anisotropy is shown to be crucial for correctly describing the shape of the local-magnetic-field distribution and associated  $\lambda_{ab}$  observed by  $\mu$ SR for field-cooled  $\text{YBa}_2\text{Cu}_3\text{O}_{7-\delta}$  powders. Since pinning is commonly present, we expect this to be a general property of the flux-line lattice in high- $T_c$  compounds. It also has important implications for related studies of magnetization,  $H_{c1}$ ,  $H_{c2}$ , flux vibration dynamics, and neutron scattering.

The authors thank C. Ballard, B. Batlogg, E. M. Gyorgy, K. Hoyle, R. N. Kleiman, L. W. Rupp, and T. Siegrist for their contributions to this work. Research at TRIUMF is supported in part by the Natural Sciences and Engineering Research Council of Canada and, through TRIUMF, by the Canadian National Research

Council.

- 
- <sup>1</sup>D. R. Nelson and H. S. Seung, Phys. Rev. B **39**, 9174 (1989).
  - <sup>2</sup>M. P. A. Fisher, Phys. Rev. Lett. **62**, 1415 (1989).
  - <sup>3</sup>S. P. Obukhov and M. Rubinstein, Phys. Rev. Lett. **65**, 1279 (1990).
  - <sup>4</sup>D. S. Fisher, M. P. A. Fisher, and D. A. Huse, Phys. Rev. B **43**, 130 (1991).
  - <sup>5</sup>P. H. Kes *et al.*, Supercond. Sci. Technol. **1**, 242 (1989).
  - <sup>6</sup>A. P. Malozemoff *et al.*, Phys. Rev. B **38**, 6490 (1988).
  - <sup>7</sup>M. Dacumling, J. M. Seuntjens, and D. C. Larbalestier, Nature (London) **346**, 332 (1990).
  - <sup>8</sup>E. H. Brandt and A. Seeger, Adv. Phys. **35**, 189 (1986).
  - <sup>9</sup>C. P. Bean, Phys. Rev. Lett. **8**, 250 (1962).
  - <sup>10</sup>E. H. Brandt, J. Low Temp. Phys. **73**, 335 (1988); Physica (Amsterdam) **162-164C**, 257 (1989); **162-164C**, 1167 (1989).
  - <sup>11</sup>D. R. Harshman *et al.*, Phys. Rev. B **36**, 2386 (1987); **39**, 851 (1989).
  - <sup>12</sup>G. J. Dolan *et al.*, Phys. Rev. Lett. **62**, 827 (1989); **62**, 2184 (1989).
  - <sup>13</sup>M. Celio *et al.*, Physica (Amsterdam) **153-155C**, 753 (1988); T. M. Riseman *et al.*, Physica (Amsterdam) **162-164C**, 1555 (1989).
  - <sup>14</sup>B. Pümpin *et al.*, Phys. Rev. B **42**, 8019 (1990).
  - <sup>15</sup>E. H. Brandt, Phys. Rev. B **37**, 2349 (1988).
  - <sup>16</sup>W. Barford and J. M. F. Gunn, Physica (Amsterdam) **156C**, 515 (1988).
  - <sup>17</sup>L. J. Campbell, M. M. Doria, and V. G. Kogan, Phys. Rev. B **38**, 2439 (1988).
  - <sup>18</sup>M. Weber *et al.*, Hyperfine Interact. **63**, 93 (1990); note, however, the distribution chosen therein is not applicable to  $\text{YBa}_2\text{Cu}_3\text{O}_7$ .
  - <sup>19</sup>H. Küpfer *et al.*, Cryogenics **28**, 650 (1988).
  - <sup>20</sup>J. C. Phillips, Phys. Rev. B **39**, 7356 (1989).
  - <sup>21</sup>A. M. Campbell and J. E. Evetts, Adv. Phys. **21**, 199 (1972).
  - <sup>22</sup>R. L. Peterson, J. Appl. Phys. **67**, 6930 (1990).